Transient response of concentrated suspensions after shear reversal

Takatsune Narumi[a)]

Department of Mechanical and Production Engineering, Niigata University, 8050 2-no-cho Ikarashi, Niigata 950-2181, Japan

Howard See

Department of Chemical Engineering, The University of Sydney, NSW 2006, Sydney, Australia

Yuichi Honma and Tomiichi Hasegawa

Department of Mechanical and Production Engineering, Niigata University, 8050 2-no-cho Ikarashi, Niigata 950-2181, Japan

Tsutomu Takahashi

Department of Mechanical Engineering, Nagaoka University of Technology, 1603-1 Kamitomioka, Nagaoka, Niigata 940-2188, Japan

Nhan Phan-Thien

School of Aerospace, Mechanical, and Mechatronic Engineering, The University of Sydney, NSW 2006, Sydney, Australia

(Received 12 July 2001; final revision received 22 October 2001)

Synopsis

We have examined the transient stress response under shear flow of concentrated suspensions of non-Brownian spheres. We focused on the experiment where the shearing is momentarily stopped and restarted in the opposite direction. We found that the normalized stress recovery curves for different values of the initial and subsequent shear rates could be collapsed quite well if plotted against the strain. This behavior agrees with the basic concept that the transient stress behavior is a function only of the imposed strain, as predicted by some recent constitutive models of concentrated suspensions. We also found that the transient behavior of the normal stress difference showed similar data collapse. Further, there appeared to be little qualitative difference in the behavior of particulate systems with a high degree of size monodispersity and those more polydisperse. © *2002 The Society of Rheology.* [DOI: 10.1122/1.1428321]

I. INTRODUCTION

Many industrial processes involve particulate suspensions, which consist of solid particles dispersed in a carrier liquid, for example paints, cosmetics, foods, filled adhesives,

[a)]Author to whom all correspondence should be addressed; electronic mail: narumi@eng.niigata-u.ac.jp

composite materials, etc. Therefore, it is most important that we continue to improve our understanding of the fundamental rheological behavior of these systems. The flow properties of suspensions are known to strongly depend on particle size, shape, volume fraction, etc., and the number of key variables make this a very challenging research field. There are summaries available in the literature of the large volume of research work that has been carried out until now [e.g., Macosko (1994); Huilgol and Phan-Thien (1997); Larson (1999)]. However, much work remains to be done, particularly towards gaining an understanding of the rheological properties of the more concentrated suspensions. Work on concentrated systems up to now has primarily focussed on the behavior under steady flow (reviewed in, e.g., Barnes 1989; Chow *et al.* 1993; Aral and Kalyon 1994; Zarraga *et al.* 2000), and much less is known about the transient behavior due to particle rearrangements at the microstructural level, which can lead to interesting structural memory effects in the mechanical response of the suspension. In this article, we focus on the particular problem of the stress recovery behavior of concentrated suspensions of spheres in a Newtonian carrier liquid under the reversal of steady shear flow. We consider systems where the particles are at least several microns in size, so the effects of Brownian motion can be assumed to be negligible.

A previous experimental study of this problem in suspension rheology was reported by Gadala-Maria and Acrivos (1980), who imposed a steady shearing with shear rate $\dot{\gamma}_i$, and observed that when the shearing was suddenly stopped, the shear stress almost instantaneously went to zero. After this stoppage, Gadala-Maria and Acrivos recommenced shearing of the sample with shear rate $\dot{\gamma}_a$, and observed the following interesting behavior: if $\dot{\gamma}_a = \dot{\gamma}_i$, so that the shearing direction was the same as that prior to the stoppage, the stress would immediately jump to the steady state value it previously had, whereas if the direction of shearing was reversed (so that $\dot{\gamma}_a = -\dot{\gamma}_i$), the stress took considerable time to rise to the steady state value. They found that the normalized shear stress recovery curves after shear reversal for different values of $\dot{\gamma}_a (= -\dot{\gamma}_i)$ could be collapsed closely to a master curve by plotting the transient behavior against shear strain $\gamma = |\dot{\gamma}_a| t$. It should be noted that Gadala-Maria and Acrivos (1980) focused on shear reversals where the initial and subsequent shear rates were of the same magnitude $|\dot{\gamma}_a / \dot{\gamma}_i| = 1$. In a subsequent work, Parsi and Gadala-Maria (1987) observed under steady shearing a "fore-and-aft" asymmetry in the particle configurations.

On the theoretical side, these results have been reproduced by the constitutive model for concentrated suspensions of non-Brownian monodisperse spheres developed by Phan-Thien and co-workers [Phan-Thien (1995); Phan-Thien *et al.* (1999, 2000)]. This approach models the motion of a generic pair of neighboring spheres in the suspension by a single pair of force-free and torque-free spheres tumbling along in the flow field. In addition, the interaction with the surrounding spheres is modeled by a diffusion-like process. The reason for the difference in the response after same direction shearing and after shear reversal is that there is a microstructure developed in the particulate under steady flow, and after sudden shear reversal it takes time for this microstructure to "flip over" and acquire the appropriate structure for the new shearing direction [Phan-Thien (1995)]. An interesting prediction of this model is that, in general, the transient stress behavior can be reduced to a function of the applied strain, meaning that the shear recovery after shear reversal should take place over a strain which is independent of the initial and subsequent shear rates. This agrees with the collapse of the normalized stress recovery curves when plotted against strain experimentally observed by Gadala-Maria and Acrivos (1980). An alternative way of expressing this strain dependence is to say that the only timescale in the physical problem is $\dot{\gamma}_a^{-1}$, a conclusion reached by Brady and Morris (1997) by microstructural scaling arguments.

TABLE I. Properties of materials used (SD = standard deviation).

	GS	MS
Particle	GP-H100 (Benzo-guanamine melamine)	MA-1010 (PMMA)
Average diameter	10 μm (SD = 0.45 μm)	6.8 μm (SD = 2.70 μm)
Specific gravity	1.4	1.2
Carrier liquid	Silicone oil 1000 cs (Specific gravity = 0.98)	
Volume fraction	$\phi = 0.4$	

While the work of Gadala-Maria and Acrivos (1980) clearly demonstrated many of the features of the shear stress recovery after shear reversal, they did not report the more general shear recovery behavior when $\dot{\gamma}_i$ and $\dot{\gamma}_a$ have different magnitudes, and it is not immediately clear from their experimental report that the behavior will show the same trends. Further, Gadala-Maria and Acrivos did not report the response of the normal stresses after shear reversal. In this article, we present experiments exploring the effect of the ratio $|\dot{\gamma}_a/\dot{\gamma}_i|$ on the transient stress recovery behavior, as well as the transient behavior of the normal stress difference N_1-N_2.

We will present results of a series of tests using microspherical particles dispersed in silicone oil, where we investigated the stress response after shear reversal with the ratio $|\dot{\gamma}_a/\dot{\gamma}_i|$ varying from 0.25 to 8.0. Our results show that the collapse of the normalized shear stress recovery curves when plotted against strain also appears to hold for the range of values of $|\dot{\gamma}_a/\dot{\gamma}_i|$, thus extending this key concept observed by Gadala-Maria and Acrivos (1980). Our conclusions are also in agreement with the theoretical predictions of the constitutive models of Phan-Thien and co-workers [Phan-Thien (1995); Phan-Thien *et al.* (1999,2000)], and Brady and Morris (1997). Further, we were able to confirm that the normal stress difference N_1-N_2 shows analogous behavior as shear stress after shear startup: if the subsequent shearing is in the same direction as the initial one, N_1-N_2 will jump instantaneously to the appropriate steady state value, whereas if the shearing direction is reversed there is a gradual rise in N_1-N_2.

This article is organized as follows. In Sec. II, we describe the materials used and the experimental setup. In Sec. III, we present the results of the rheological tests and in Sec. IV, we discuss the stress recovery behavior in terms of the theoretical models.

II. EXPERIMENTAL

Two types of spherical particles were used: MA-1010 (Nippon Shokubai Co., Ltd., Japan) were particles made of poly(methyl methacrylate) (PMMA); GP-H100 (Nippon Shokubai Co., Ltd., Japan) were particles made of Benzo-guanamine melamine. Table I gives further details of the particles. Note that the GP-H100 particles were highly monodisperse in size, while the MA-1010 particles had a degree of size variability. The particles were dispersed in a silicone oil with viscosity 1.13 Pa s at 20 °C and specific gravity of 0.98 (Shin-Etsu Chemical Co., Ltd., Japan). Thorough hand mixing and 30 min of ultrasonic vibration and defoaming were carried out to ensure that the particles were uniformly dispersed in the suspension—no clumping or sedimentation of the particles was observed. In this article, we label the suspension with MA-1010 particles as "MS" and that with GP-H100 particles as "GS," as shown in Table I. Our focus was on the behavior of systems with reasonably high concentrations, so the volume fraction was fixed at $\phi = 0.4$. The measurements were conducted at temperatures of 20 °C–25 °C.

The rheometer was a Rheometrics Scientific ARES system in the parallel plate configuration with 50 mm plate diameter and 1 mm gap. This configuration was used since we also wished to measure the transient behavior of the normal stress difference N_1-N_2. Despite the fact that the shear rate is not uniform over the sample, the standard inversion procedure (Macosko, 1994) allows the shear stress at the rim shear rate $\dot{\gamma}_R$ to be established in terms of the torque M,

$$\tau(\dot{\gamma}_R) = \frac{M}{2\pi R^2}\left[3+\frac{1}{2\pi R^2}\frac{d(\ln M)}{d\dot{\gamma}_R}\right], \tag{1}$$

where R is the radius of the plate. For systems where there is little or no shear thinning, as is the case here, the transient response of the measured torque is the transient response of the shear stress at shear rate $\dot{\gamma}_R$. The cone-plate configuration was not used because of difficulties experienced in achieving the initial gap setting without residual thrust, which is a common problem when working with suspensions containing particles several microns in size or larger. In all tests, the preshear flow was applied to the test fluid for 30 s at a constant shear rate $\dot{\gamma}_i$ ($\dot{\gamma}_i$ = 0.25–2 s^{-1} was the range used, and the shear rate refers to the value at the outer radius of the plate). The flow was stopped and then the shearing was immediately applied in the opposite direction with constant shear rate $\dot{\gamma}_a$, and the transient stress responses recorded. This procedure was carried out for several values of the shear rate ratio $|\dot{\gamma}_a/\dot{\gamma}_i|$. Simultaneously, the transient behavior of the normal stress difference N_1-N_2 was determined from the normal force acting on the parallel plates. We confirmed that the results showed reasonable reproducibility. For comparison, steady shear stress measurements were made with a HAAKE RS-50 rheometer in the parallel plate configuration with 35 mm plate diameter and 1 mm gap. The HAAKE tests were also carried out for more than 30 s, which was found to be sufficient time for the viscosities to reach steady state values for the range of shear rates studied. At the conclusion of each test, the upper plate was carefully lifted and the sample inspected. There did not appear to be significant settling or separation of the dispersed particles.

III. RESULTS

Figure 1 illustrates the steady shear response of the samples. The data shown was obtained after prolonged shearing following shear reversal with the ARES (τ_s in Fig. 3). Also plotted for comparison are the steady values measured with the RS-50. From Fig. 1, we see that there is good agreement between the two rheometers. Further, we see that the 30 s of prolonged shearing after shear reversal on the ARES was of sufficient duration for the system to reach steady state in our test conditions. It should be noted that over the shear rate range studied, the fluids were observed to be slightly shear thinning and to have a very small yield stress, but the behavior was still sufficiently close to Newtonian to justify the simplified theoretical treatment to be discussed later.

When the direction of the subsequent shearing was the same as the preshearing, we observed for all values of the ratio $|\dot{\gamma}_a/\dot{\gamma}_i|$ that the shear stress recovers immediately to the steady state value. The upper plot in Fig. 2 shows one of the stress response curves in this case. For the experiments where the shear direction was reversed, we indeed found that the stress shows a gradual recovery (lower plot in Fig. 2), in agreement with the report of Gadala-Maria and Acrivos (1980). The plots in Fig. 2 show a pause time, but we found that the stress responses in the subsequent flow were independent of the duration of the pause time. Hence, further tests were conducted with no pause time, as shown in Fig. 3. We use Fig. 3 to define the following key physical quantities in the shear reversal experiment: τ_j is the magnitude of the initial recovery in the shear stress, τ_s is the steady

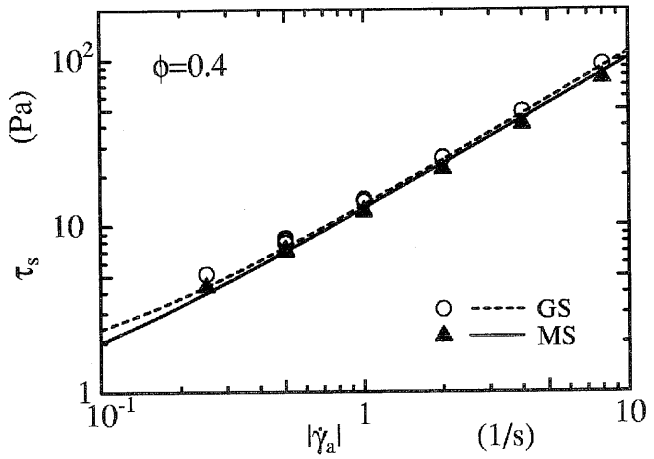

FIG. 1. Steady shear stress measured with the parallel plates. The data points were obtained using ARES with prolonged shearing after shear reversal, and the lines were obtained using HAAKE RS-50 with steady shear flow (shown for comparison).

state value, and t_{95} is a characteristic rise time—the time taken for the shear stress to reach 95% of the steady state value. Using t_{95}, we can define a corresponding strain $\Gamma_{95} = |\dot{\gamma}_a| t_{95}$. To determine τ_j, as indicated in Fig. 3, the local plateau value is used, since the "peak" which exists before that may be influenced by the mechanical properties of the rheometer. These parameters will be used to quantify the degree of data collapse from the various shear response tests performed.

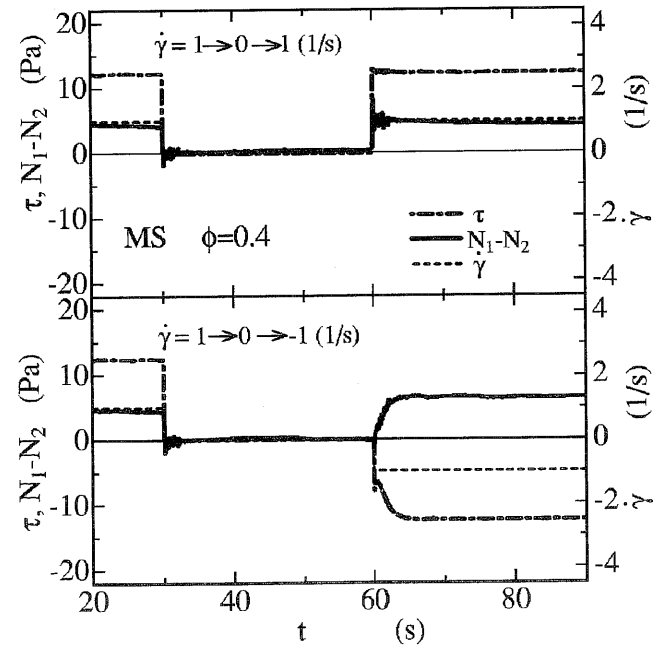

FIG. 2. Typical stress responses in restarted flow with a pause time. The upper plot shows subsequent flow in the same direction as the preflow, the lower plot shows the behavior after flow reversal.

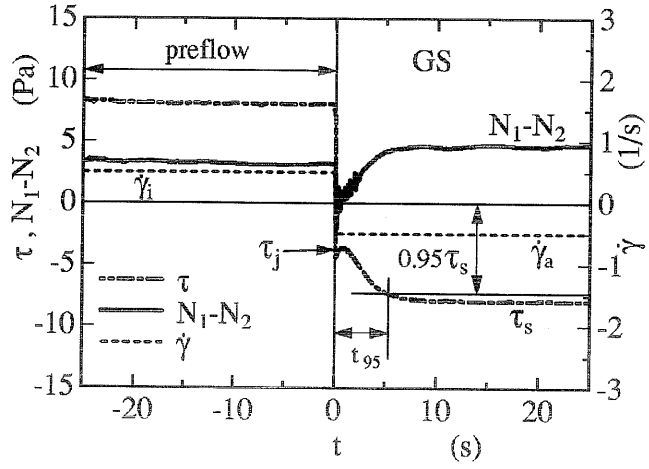

FIG. 3. Typical stress response curves obtained with no pause time, indicating the notations used in the present article.

Figure 4 shows the values of the ratio τ_j / τ_s versus the ratio of the initial and subsequent shear rates $|\dot{\gamma}_a / \dot{\gamma}_i|$ for the series of shear reversal experiments. We notice that the values are quite close over the range of $|\dot{\gamma}_a / \dot{\gamma}_i|$, indicating that although the values of the stresses may depend on the shear rates as one would expect, the essential shape of the response curves are the same.

Similarly, Fig. 5 shows the characteristic response strain Γ_{95} as a function of the ratio $|\dot{\gamma}_a / \dot{\gamma}_i|$. We see again that the values are very similar, indicating that when the various shear stress recovery curves are plotted as a function of strain, there is good collapse of the data. Further, in Figs. 4 and 5, we observe that there is little difference between the results for the highly monodisperse system (GS) and the more polydisperse suspensions (MS).

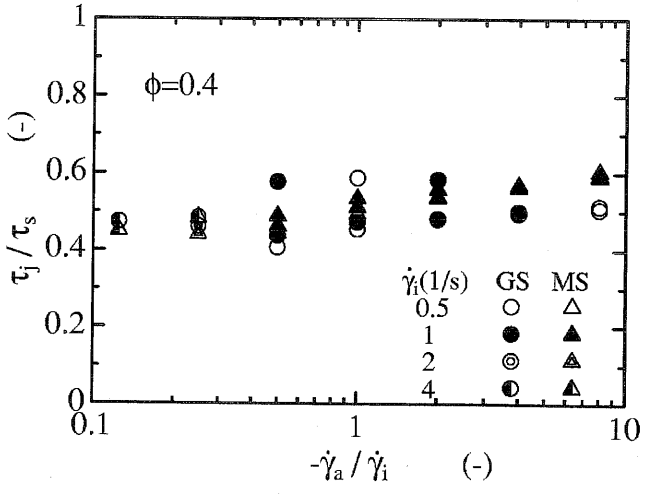

FIG. 4. Shear stress recovery τ_j (normalized by the final steady value τ_s) immediately after flow reversal, as a function of shear rate ratio.

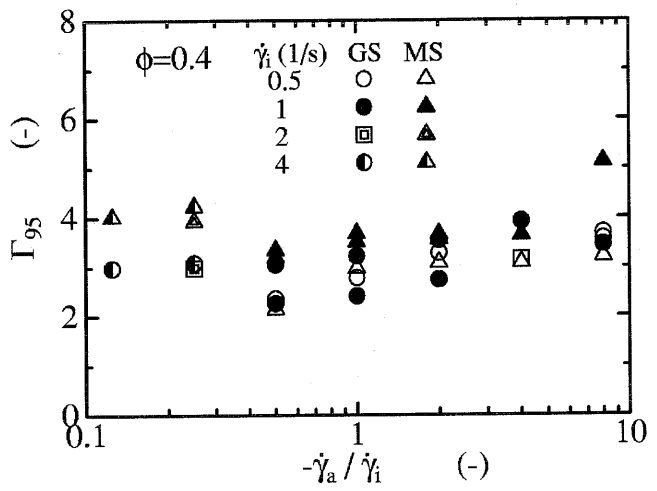

FIG. 5. Strain corresponding to the 95% of shear stress recovery in the flow reversal experiment, as a function of shear rate ratio.

Typical response curves for the normal stress difference N_1-N_2 after the stopping and starting of shearing in the same direction and for the case of shear reversal are also shown in Fig. 2. Similar to the shear stress, we see that N_1-N_2 rises almost instantaneously to the steady value when flow is restarted in same direction, whereas a gradual growth with no partial jump is observed in the case of flow reversal. The steady values of $(N_1\text{-}N_2)_s$ are illustrated in Fig. 6. We observe that this quantity is positive for all cases considered, and that the dependence on shear rate $\dot{\gamma}_a$ parallels that of the shear stress (also plotted as lines on Fig. 6 for comparison). It should be noted that, because of the difficulty in the initial setting as mentioned in Sec. II, these normal stress values may contain appreciable error (our estimate is 20%–30% at most). From Fig. 6, it is seen that the ratio $(N_1\text{-}N_2)_s/\tau_s$ is approximately 0.5 over the shear rate range studied. This is somewhat larger than the values obtained by Zarraga *et al.* (2000) in their steady shearing tests on

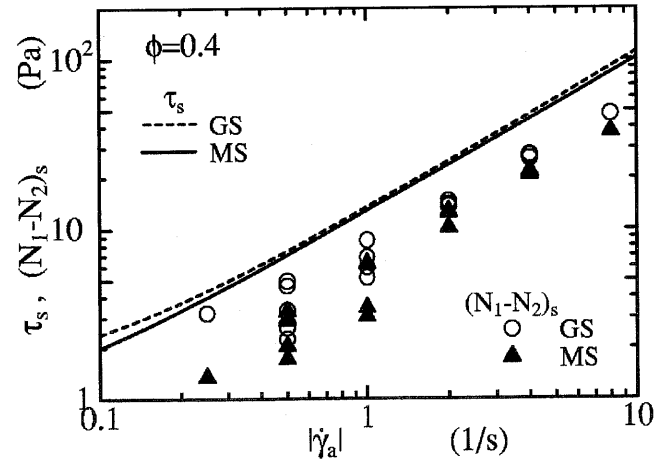

FIG. 6. Steady state values of the normal stress difference N_1-N_2 (data points) and shear stress (lines) as a function of shear rate. The similarity in shear rate dependence of these quantities can be observed.

suspensions of glass spheres, which had an average size of 43 μm and were quite polydisperse. It is perhaps not unexpected that the monodisperse GS system may generate a high normal stress effect due to a highly arranged microstructure. However, the reason for the difference in $(N_1\text{-}N_2)_s/\tau_s$ values between the MS system and the glass spheres is unclear at present, and more precise measurements of the normal stress difference are certainly needed.

Figures 7(a) and 7(b) show the growth of $(N_1\text{-}N_2)$ normalized with the steady value for the GS sample for several combinations of $\dot{\gamma}_a$ and $\dot{\gamma}_i$. We see that the $N_1\text{-}N_2$ recovery curves collapse well to a master curve for all cases. Figure 7(c) shows similar curves obtained for the polydisperse suspension (MS) and we again see the data collapse to a master curve, paralleling the behavior observed in the GS system. Thus, it is apparent that this data collapse occurs not just for shear stress but also for the normal stress difference $N_1\text{-}N_2$.

IV. DISCUSSION

To facilitate comparison between the experimental observations and the theory, we now briefly introduce the key points of the constitutive model for concentrated suspensions of monodisperse spheres in a Newtonian carrier fluid, recently developed by Phan-Thien and co-workers [Phan-Thien (1995); Phan-Thien *et al.* (1999, 2000)]. The essential idea is that the motion of a neighboring pair of generic spheres in the suspension is modeled by a single pair of force-free and torque-free spheres, which tumble along with the imposed flow field. It is convenient to introduce $\mathbf{p}$, the unit vector field directed between the particle centers. Since the suspension is concentrated, each sphere experiences interactions with surrounding spheres, and this effect is modeled by an anisotropic diffusion-like process, with the magnitude of the diffusion tensor $\mathbf{D}_r$ assumed to be proportional to the imposed rate of strain. The following formula for the instantaneous particle-contributed stress tensor τ_p is obtained (Phan-Thien *et al.* 1999)

$$\tau_p = \mu(\phi)[(1-\xi)\mathbf{D}:\mathbf{A}_2 + \dot{\gamma}(\mathbf{K}\cdot\mathbf{A}_2 + \mathbf{A}_2\cdot\mathbf{K} + tr(\mathbf{K})\mathbf{A}_2 - 2\mathbf{K}:\mathbf{A}_4)]. \tag{2}$$

Here, $\mu(\phi)$ is a scalar viscosity depending on the volume fraction ϕ, ξ is a hydrodynamic interaction factor ($\xi = 0.63$ for highly concentrated monodisperse spheres), $\mathbf{D}$ is the strain rate tensor, and $\dot{\gamma}$ is a measure of the rate of strain $\dot{\gamma} = \sqrt{2tr(\mathbf{D}\cdot\mathbf{D})}$. $\mathbf{K}$ is a dimensionless tensor, which plays the constitutive role of describing the degree of anisotropy of the diffusion process—it is assumed $\mathbf{D}_r = \dot{\gamma}\mathbf{K}$. $\mathbf{A}_2$ and $\mathbf{A}_4$ are tensors which describe the system microstructure: $\mathbf{A}_2 = \langle\mathbf{pp}\rangle$ and $\mathbf{A}_4 = \langle\mathbf{pppp}\rangle$.

In transient flows, the system microstructure develops through the time evolution equations for $\mathbf{A}_2$ and $\mathbf{A}_4$. For example, the equation describing the change in $\mathbf{A}_2$ is

$$\frac{d\mathbf{A}_2}{dt} = (\boldsymbol{L}-3\dot{\gamma}\mathbf{K})\cdot\mathbf{A}_2 + \mathbf{A}_2\cdot(\boldsymbol{L}-3\dot{\gamma}\mathbf{K})^T - 2(\boldsymbol{L}-3\dot{\gamma}\mathbf{K}):\mathbf{A}_4 + 2\dot{\gamma}\mathbf{K} - 2\dot{\gamma}tr(\mathbf{K})\mathbf{A}_2 \tag{3}$$

where $\boldsymbol{L}$ is an equivalent velocity gradient tensor $\boldsymbol{L} = \mathbf{L} - \xi\mathbf{D}$, with $\mathbf{L}$ the velocity gradient tensor of the imposed flow field and ζ a hydrodynamic parameter ($\zeta = 0.13$). Note that the right-hand side of Eq. (3) involves the fourth-order tensor $\mathbf{A}_4$—to analytically deal with this equation, a closure approximation is often employed (e.g., quadratic closure $\mathbf{A}_4 \cong \mathbf{A}_2\mathbf{A}_2$).

We observe that the right-hand side of Eq. (3) is linear in the rate of strain $\dot{\gamma}$. This means that during transient response, the timescales for structural evolution and, hence,

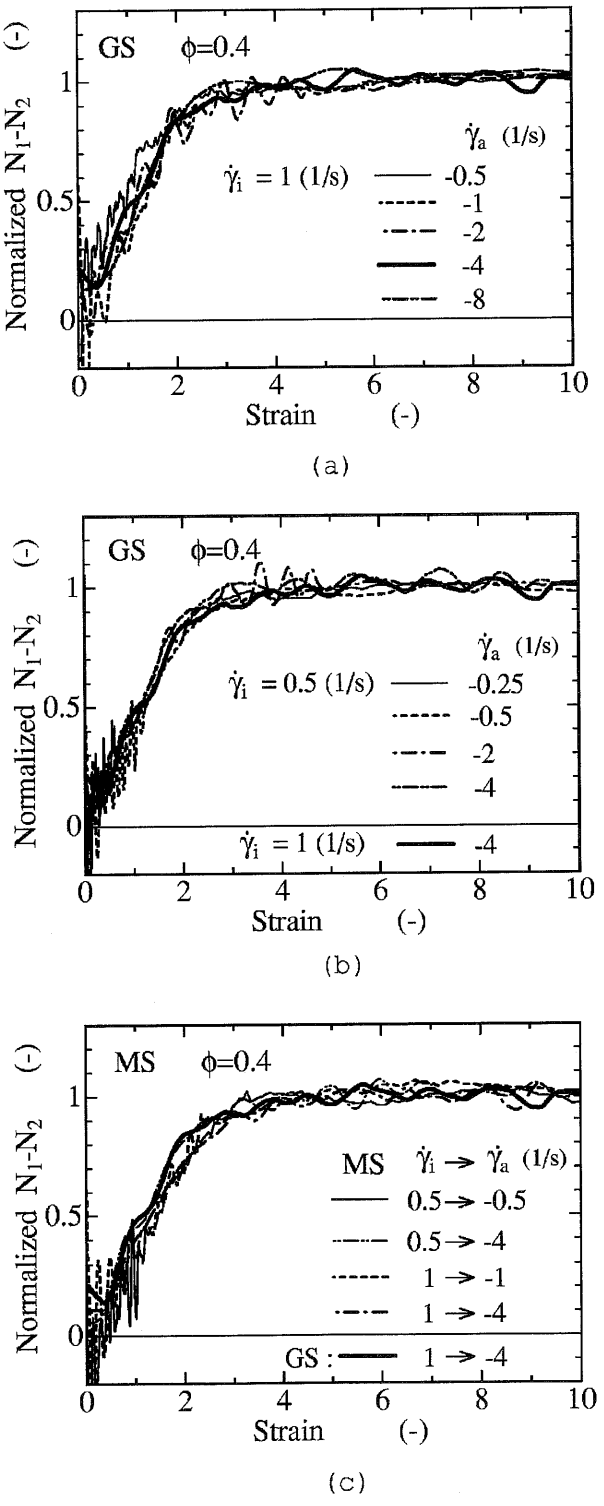

FIG. 7. Recovery of $(N_1\text{-}N_2)$ normalized with the steady value after flow reversal. (a) $\dot{\gamma}_i = 1$ (1/s) and (b) $\dot{\gamma}_i = 0.5$ (1/s) are obtained with GS, and (c) is measured with the MS system. To facilitate comparison, the line for the case of $\dot{\gamma}_i = (1/s)$ and $\dot{\gamma}_a = -4(1/s)$ with the GS sample is shown.

the stress tensor evolution must be inversely proportional to $\dot{\gamma}$—in other words, the microstructure and stresses evolve only as a function of the imposed strain. A similar conclusion has also been reached by Brady and Morris (1997) via scaling arguments.

We now discuss our experimental results in the light of this constitutive framework. We observed experimentally that the shear stress and normal stress difference (Fig. 2) instantaneously jumped to the appropriate steady state values if the shearing is recommenced in the same direction. This behavior agrees with Eqs. (2) and (3), since, if after prolonged shearing, the shear flow is restarted in the same direction (even with a different magnitude of the shear rate), the right-hand side of Eq. (3) will still remain zero. To see this, note that the right-hand side would have evolved to zero after prolonged shearing and that it is linear in the shear rate. Hence, when the subsequent flow with the same structure tensor restarts in the same direction, the right-hand side of Eq. (3) remains zero and there will be no change in the structure tensors. Therefore, by Eq. (2), the shear and normal stresses will immediately jump to the new steady state values corresponding to the applied shear rate.

On the other hand, if the shearing direction is reversed, there will be an evolution of microstructure determined by Eq. (3), and this will cause a gradual change in the stress tensor via Eq. (2). It should be noted that immediately after shear reversal, Eq. (2) predicts that the shear stress recovers only partially before evolving to the new steady state (since $\mathbb{D}$ changes sign but $\dot{\gamma}$ does not), as observed in our tests (Fig. 3). Equation (3) tells us that the evolution of the structure will be a function only of the imposed strain $\gamma = |\dot{\gamma}_a|t$. This means that if the components of the normalized stress tensor are plotted as a function of γ, their time evolution (or recovery curves) will collapse to a common curve, even for different values of the ratio $|\dot{\gamma}_a/\dot{\gamma}_i|$. In our experiments, we succeeded in observing these behaviors for both the shear stress and the normal stress recovery curves (Figs. 4, 5, and 7). Indeed, we notice that the strain for $(N_1\text{-}N_2)$ to reach the steady state is similar to the strain for the shear stress to reach the steady state after shear reversal.

Although a direct qualitative comparison between this constitutive model and experiments requires knowledge of the key quantities $\mu(\phi)$ and $\mathbb{K}$, the strain to reach steady state after shear reversal has been theoretically predicted to be close to 1 [Phan-Thien (1995), using $\mathbb{K} = 2.5\,\mathbb{1}$, where $\mathbb{1}$ is the unit tensor]. This is somewhat lower than the present results (Γ_{95} in Figs. 5, and 7), indicating that while the model appears capable of capturing many of the essential physics of the problem, quantitative agreement will probably require a more sophisticated theoretical framework.

V. CONCLUSIONS

We have carried out a series of rheological tests on concentrated suspensions of non-Brownian particles, with particular focus on the stress recovery behavior after the shear flow is momentarily stopped and restarted in the opposite direction. We found that for the range of initial and subsequent shear rates investigated, there was good collapse of the data if the normalized stress recovery curves were plotted against strain. Further, we found that the recovery curves for the normal stress difference $N_1\text{-}N_2$ (appropriately normalized) also showed good collapse of data if plotted against the strain. These results extend the observations made in the pioneering experiments of Gadala-Maria and Acrivos (1980).

Our results are in good qualitative agreement with the theoretical predictions of a recent constitutive model for concentrated suspensions developed by Phan-Thien and co-workers [Phan-Thien (1995); Phan-Thien *et al.* (1999, 2000)]. This suggests that the core idea of this formulation, where the particle–particle interactions are modeled as a

strain-rate dependent diffusion-like process, is possibly quite close to capturing the essential physics of the flow behavior of concentrated suspensions.

Interestingly, our experiments show that polydispersity in particle size does not appear to have a major effect on the data collapse, suggesting that modifications to the existing constitutive framework may yield models which could be fruitfully applied to these systems as well. However, it should be noted that the degree of polydispersity in the MS system is not that large, and thus these results should be regarded as somewhat preliminary. There is a need for a systematic investigation of the effects of polydispersity on these response phenomena, for example using a bimodal system with widely differing particle sizes.

Concentrated suspensions are a very important class of materials in industry, and an understanding of their flow behavior is essential for optimizing their processability and function. It is hoped the present work has shed some light on the transient flow behavior of these systems.

ACKNOWLEDGMENT

The authors gratefully acknowledge the help of Atsushi Suzuki in the experimental stages of this project.

References

Aral, B. K. and D. M. Kalyon, "Effects of temperature and surface roughness on time-dependent development of wall slip in steady torsional flow of concentrated suspensions," J. Rheol. **38**, 957–972 (1994).

Barnes, H. A., "Shear-thickening ("Dilatancy") in suspensions of non-aggregating solid particles dispersed in Newtonian liquids," J. Rheol. **33**, 329–366 (1989).

Brady, J. F. and J. Morris, "Microstructure of strongly sheared suspensions and its impact on rheology and diffusion," J. Fluid Mech. **348**, 103–139 (1997).

Chow, A. W., S. W. Sinton, and J. H. Iwamiya, "Direct observation of particle microstructure in concentrated suspensions during the falling-ball experiment," J. Rheol. **37**, 1–16 (1993).

Gadala-Maria, F. and A. Acrivos, "Shear-induced structure in a concentrated suspension of solid spheres," J. Rheol. **24**, 799–814 (1980).

Huilgol, R. R. and N. Phan-Thien, *Fluid Mechanics of Viscoelasticity* (Elsevier, Amsterdam, 1997), pp. 239–270.

Larson R. G., *The Structure and Rheology of Complex Fluids* (Oxford University Press, Oxford, 1999), pp. 261–323.

Macosko, C. W., *Rheology: Principles, Measurements, and Applications* (VCH, New York, 1994), pp. 424–475.

Parsi, F. and F. Gadala-Maria, "Fore-and-aft asymmetry in a concentrated suspension of solid spheres," J. Rheol. **31**, 725–732 (1987).

Phan-Thien, N., "Constitutive equation for concentrated suspensions in Newtonian liquids," J. Rheol. **39**, 679–695 (1995).

Phan-Thien, N., X. J. Fan, and B. C. Khoo, "A new constitutive model for monodispersed suspensions of spheres at high concentrations," Rheol. Acta **38**, 297–304 (1999).

Phan-Thien, N., X. J. Fan, and R. Zheng, "A numerical simulation of suspension flow using a constitutive model based on anisotropic interparticle interactions," Rheol. Acta **39**, 122–130 (2000).

Zarraga, I. E., D. A. Hill, and D. T. Leighton, "The characterization of the total stress of concentrated suspensions of noncolloidal spheres in Newtonian fluids," J. Rheol. **44**, 185–220 (2000).